Miscibility Study in Fluorinated Tetrafluoroethylene Copolymer−Copolymer Blends†

Rachele Pucciariello* and Vincenzo Villani

Dipartimento di Chimica, Universita' della Basilicata, Via N. Sauro 85, 85100 Potenza, Italy

Odda Ruiz de Ballesteros

Dipartimento di Chimica, Universita'di Napoli Federico II, Via Mezzocannone 4, 80134 Napoli, Italy

Received July 6, 2000; Revised Manuscript Received December 13, 2000

ABSTRACT: The miscibility of random fluorinated tetrafluoroethylene copolymers is investigated by differential scanning calorimetry (DSC) and X-ray diffraction (XRD). In particular, mixtures composed of poly(tetrafluoroethylene)-*co*-(hexafluoropropylene) (FEP) containing 1 mol % of comonomer and poly-(tetrafluoroethylene)-*co*-(perfluoromethylvinyl ether) (PFMVE) containing from 2 to 10 mol % of comonomer have been examined. The miscibility has been found to depend more upon the difference in the defect (counit) concentration between the two components than upon the blend composition and the crystallization conditions.

Introduction

Polymer blends have gained an increasing interest in both industrial and scientific fields. These studies are largely concerned with amorphous/amorphous[1,2] or amorphous/semicrystalline blends,[3−5] and just a few studies concern semicrystalline/semicrystalline polymer blends, for example, those of different grade polyethylene,[6−10] poly(vinylfluoride) and poly(vinylidenfluoride),[11−12] vinylidenfluoride−trifluoroethylene copolymers,[13] poly-(tetrafluoroethylene) and poly(tetrafluoroethylene-*co*-perfluoro-*n*-propylvinyl ether).[14] Nevertheless, the blends in which both components are semicrystalline are particularly important for either the large diffusion of semicrystalline polymers or the way in which the crystallinity of one component influences the crystallization of the other. In particular, the possibility that the two components crystallize together in a single-crystal lattice (cocrystallization) is very important. It is a rare phenomenon, since it requires close matching of chain conformations and of lattice symmetry and dimensions, in addition to similar crystallization kinetics.

For crystalline homopolymer−copolymer or copolymer−copolymer blends, it has been shown that the phase behavior strongly depends on the difference in counit concentration, as well as upon the blend composition and the crystallization conditions. For example, some authors reported that linear and branched poly(ethylene) do not produce cocrystals at all compositions[9,15−17]. On the other hand, Galante et al.[18] showed that linear and branched polyethylenes are able to cocrystallize, depending upon the closeness of the crystallization rates of each component, the copolymer composition and molecular structure, and the crystallization conditions. For blends of poly(vinylidenfluoride) and poly(vinylidenfluoride-*co*-tetrafluoroethylene), it was reported that cocrystallization depends on the difference in $-CF_2-CF_2-$ defect; only if such difference is low can cocrystallization take place at all compositions and temperature. Otherwise, it strongly depends on crystallization temperature;[19,20] a similar behavior is observed for blends of poly(vinylidenfluoride) and poly(vinylidenfluoride-*co*-trifluoroethylene).[13]

In a previous paper,[21] we investigated the phase behavior of binary crystalline blends obtained by melt-mixing of random fluorinated copolymers of tetrafluoroethylene, i.e. with hexafluoropropylene at 1 mol % comonomer (FEP copolymer) and perfluoromethylvinyl ether at 2 mol % comonomer (PFMVE copolymer). Study by differential scanning calorimetry (DSC) of melting, crystal−crystal transitions, and crystallization indicates the occurrence of cocrystallization for almost all compositions and all investigated experimental conditions.

In the present work, we extend the previous study to other blends in order to define the most important parameters governing the possibility of cocrystallization. Blends composed of FEP (1 mol % comonomer) and PFMVE at comonomer concentrations in the range 4−10 mol % have been characterized to evaluate the influence of the difference in defect content on the phase behavior of the blends. The polymers used for the blend preparation are both crystallizable and readily undergo crystallization from the melt in the pure state. Their melting, crystallization, and crystal−crystal transitions (when present) are sufficiently different to allow discriminating univocally the occurrence or not of cocrystallization.[22−26]

The study has been performed by differential scanning calorimetry in order to detect the presence of single or multiple transition at melting, crystallization, and polymorph transitions.

X-ray diffraction measurements (XRD) have been carried out to evaluate eventual structural changes which may be related to the occurrence of cocrystallization.

Experimental Section

Materials. Powder samples of FEP and PFMVE were used. Their characteristics are reported in Table 1. They were obtained by conventional aqueous dispersion polymerization. The comonomer concentrations ranging from 1 to 10 mol % were determined by the infrared analytical method.[27]

* E-mail: Pucciariello@unibas.it.

† Dedicated to Professor Paolo Corradini on the Occasion of his 70th Birthday.

10.1021/ma001172j CCC: $20.00
Published on Web 02/10/2001

Table 1. Samples Used in the Preparation of the Blends

sample	comonomer	comonomer content (mol %)
FEP	CF_2=CF(CF_3)	1
PFMVE2	CF_2=CF(OCF_3)	2
PFMVE4	CF_2=CF(OCF_3)	4
PFMVE6	CF_2=CF(OCF_3)	6
PFMVE10	CF_2=CF(OCF_3)	10

The blends were prepared by physically and intimately mixing the powders, then taking them to melt at 350 °C, holding them at this temperature for 1 min (we have verified that longer times at this temperature do not affect the subsequent thermal behavior), and then cooling them to room temperature (heating and cooling were performed at 10 °C/min, unless otherwise specified).

The blend compositions are reported as weight fractions of FEP (w_{FEP}).

All of the examined blends with their thermal properties are reported in Tables 2−4.

Thermal Analysis. Thermal analysis was performed by a differential scanning calorimeter (DSC 7, Perkin-Elmer). Runs were performed on 5.0 ± 0.5 mg samples in a nitrogen atmosphere. The apparatus was calibrated using the melting temperatures of mercury (−38.9 °C), indium (156.6 °C), and lead (327.4 °C) and their heats of fusion. Before each run, the baseline was optimized in the suitable temperature range (from 200 to 350 °C, from 350 to 200 °C, and from −30 to +50 °C, as required in the subsequent experiment) and subtracted from the corresponding DSC curve. Transition temperatures were taken as the appropriate peak temperatures in the DSC curves and are reproducible to ±0.5 °C. The heats of transition were calculated from the peak areas by the Pyris software running under Windows NT 3.51 on a Compaq Prolinea 5133 computer, and their uncertainty is ±0.3 J g^{-1}.

The runs were performed at 10 °C/min.

The quenching was carried out in the DSC apparatus by cooling the sample from the melt to −35 °C at 80 °C/min.

Due to the different thermal behavior of the considered polymers when native or melt-crystallized,[22,25,26] all of the reported calorimetric curves of neat components concern the melt-crystallized samples.

X-ray Diffraction. Structural characterizations were conducted at room temperature where all of the copolymers involved in the blend are in the less-ordered crystalline phase I (pseudohexagonal). The X-ray diffraction photographs were obtained on a BAS-MS imaging plate (Fujifilm) using a flat-plate camera with Ni-filtered Cu Kα radiation (λ = 1.5418 Å). Nonmelted powder samples were put in a Lindemann capillary (1.5 mm diameter). Then, the capillary was put in the DSC pan, and the sample was allowed to melt from 200 to 350 °C at 10 °C/min, taken for 1 min at 350 °C, and then cooled to room temperature at 10 °C/min. At this point, the capillary was removed from the DSC pan and mounted vertically on the specimen in the flat-camera, using a distance sample-film of 10 mm and an exposure time of 60 min.

The photographs were processed with a digital imaging reader (Fujibas 1800) to obtain the patterns of intensity as a function of 2θ. In particular, the intensity is calculated by averaging the measurements along the equator and the meridian. The uncertainty on 2θ is ± 0.05°.

The angular half-height widths (β) of the (100) diffraction peak have been evaluated by the Gaussian fitting and have been used to calculate the correlation length D of the crystalline domains in the directions perpendicular to the chain axes using the Scherrer formula:

$$D = k\lambda/\beta \cos \theta$$

where k is a constant that is commonly assigned a value of 0.9.

Results

Thermal Analysis. In Figures 1−3, the melting, crystallization, and crystal−crystal transition DSC curves are reported for the examined blends. The corresponding curves for the unblended polymers are also reported for the sake of comparison.

The melting endotherms for the blend FEP/PFMVE4 (Figure 1A) show a dominant peak at a temperature decreasing upon increasing PFMVE4 content in the blend, being always located at temperatures lower than the melting of unblended FEP (Table 2). Anyway, there is evidence of a second small endotherm, strongly increasing upon increasing PFMVE4 content, at temperatures slightly below that of neat PFMVE4 melting peak, but corresponding to the lower temperature portion of PFMVE4 endotherm.

Also, the blend FEP/PFMVE6 (Figure 1B) shows a main melting peak occurring at decreasing temperatures on increasing the content of PFMVE6, and another smaller peak located at a temperature slightly below than that of neat PFMVE6 (Table 3). However, the temperature of the higher melting peak is less affected by the blend composition than in the previous case; in fact, it decreases to a lesser extent as a function of the low-melting component content. The trend of the lower peak temperature is similar to that observed for the blend FEP/PFMVE4, being always slightly below than in the neat polymer. Anyway, this peak is more intense than in the previous case.

In contrast, for the blend FEP/PFMVE10 (Figure 1C), a peak can be observed corresponding to the melting of unblended FEP but not dependent upon the blend composition. Nevertheless, this peak presents a very long tail toward the low-temperature range, which appears as a well-defined shoulder at w_{FEP} = 0.75. It is worth noting that the peak corresponding to PFMVE10 melting is very broad (it has a very large temperature interval) and is scarcely appreciable even in the unblended component, due to its poor crystallinity.

As far as crystallization is concerned, for the blend FEP/PFMVE4 (Figure 2A), a largely dominant exotherm is observed always at temperatures lower than that of crystallization of unblended FEP and decreasing with increasing PFMVE4 content. A very small exotherm appears starting from w_{FEP} = 0.50 at higher temperatures than that of the peak of crystallization of neat PFMVE4, whose peak slightly decreases (1 °C) on increasing PFMVE4 content, and it is always higher than that of neat PFMVE4.

As for melting, the crystallization curves of FEP/PFMVE6 (Figure 2B) blend also show a dominant exotherm occurring at higher temperature and a smaller peak at lower temperatures, increasing in extent and decreasing in value on increasing PFMVE6 content. Also, the higher temperature peak increases on increasing PFMVE6 content. The higher peak temperature is less affected by the blend composition than that in the blend with PFMVE4, the lower is always above the crystallization temperature of neat PFMVE6.

For the blend FEP/PFMVE10 (Figure 2C) at each composition, one crystallization peak is observed at about the same temperature as that in unblended FEP. As for the melting, the crystallization peak of PFMVE10 is not appreciable.

Last, let us consider the crystal−crystal transitions. We wish to remind the reader that for melt-crystallized PTFE two crystal−crystal transitions take place close to room temperature corresponding to the triclinic−hexagonal and hexagonal−pseudohexagonal transitions.[28,29] For FEP copolymers, they are shifted toward

Table 2. Heats and Transition Temperatures of the Blend FEP/PFMVE4

composition (weight fraction of FEP, W_{FEP})	T_t (°C)		ΔH_t (J g^{-1})[a]	T_m (°C)		ΔH_m (J g^{-1})[a]	T_c (°C)		ΔH_c (J g^{-1})[a]
FEP−PFMVE4									
1.0		4.8 16.6	9.1		318.8	62.2		299.7	54.9
[b]		7.3 17.1	8.3		321.7	61.5			
0.75	−9.4[c]	4.5 15.8	6.3	284.5[c]	317.5	40.1	268.9[c]	299.7	44.5
[b]	−8.8[c]	4.2 15.6[c]	5.8	284.3[c]	316.0	38.6			
0.50	−9.7	3.2 12.3[c]	4.2	283.5	314.8	28.5	268.8	294.2	28.5
[b]	−11.7[c]	3.2 12.1[c]	4.1	283.5	315.5	31.6			
0.25	−11.7	3.2 11.3[c]	1.8	282.8	311.2	18.3	267.8	289.7	14.3
[b]		−1.2 11.3	1.0	280.8	306.0	17.2			
0.0	−13.2		1.2	287.8		14.3	262.3		15.7
	−14.7		0.8	288.0		14.4			

[a] Total heat of transition. [b] After *quenching*. [c] Very small shoulder of the main peak.

Table 3. Heats and Transition Temperatures of the Blend FEP/PFMVE6

composition (weight fraction of FEP, W_{FEP})	T_t (°C)		ΔH_t (J g^{-1})[a]	T_m (°C)		ΔH_m (J g^{-1})[a]	T_c (°C)		ΔH_c (J g^{-1})[a]
FEP−PFMVE6									
1.0	4.8	16.6	9.1		318.8	62.2		299.7	54.9
[b]	7.3	17.1	8.3		321.7	61.5			
0.75	4.2	15.5	6.6	267.0	317.7	50.2	251.8	299.5	56.5
[b]	3.5	16.6	5.7	265.8	315.7	46.3			
0.50	3.3	15.0	4.7	266.5	315.7	34.4.	252.3	297.8	35.8
[b]	4.1	14.6	4.9	265.8	317.5	36.9			
0.25	3.5	12.4	1.7	266.5	314.0	13.8	252.8	299.5	19.5
[b]	2.33	12.9	1.22	266.0	314.5	16.0			
0.0				269.0		11.8	244.5		12.4
				271.0		13.9			

[a] Total heat of transition. [b] After *quenching*. [c] Very small shoulder of the main peak.

Table 4. Heats and Transition Temperatures of the Blend FEP/PFMVE10

composition (weight fraction of FEP, W_{FEP})	T_t (°C)		ΔH_t (J g^{-1})[a]	T_m (°C)		ΔH_m (J g^{-1})[a]	T_c (°C)		ΔH_c (J g^{-1})[a]
FEP−PFMVE10									
1.0	4.8	16.6	9.1		318.8	62.2		299.7	54.9
[b]	7.3	17.1	8.3		321.7	61.5			
0.75	5.3	17.7	2.9		318.2	37.6		301.3	28.4
[b]	5.2	17.8[c]	3.1		318.2	32.5.			
0.50	5.7	18.0	3.6		320.3	28.0		301	31.4
[b]	5.50	17.6	3.3		319.3	28.8			
0.25	5.50	17.7	1.8		320.3	14.2		301	16.9
[b]	5.7	17.8	1.3		319.	15.3			
0.0				225.0		2.32	206.3		5.7
				231.6		1.02			

[a] Total heat of transition. [b] After *quenching*. [c] Very small shoulder of the main peak.

lower and lower temperatures on increasing the comonomer content, merging to only one at higher counit concentrations,[30] whereas for the PFMVE copolymer, only one transition is observed at lower temperatures, which disappears for comonomer contents larger than 4 mol %.[22]

For the blend FEP/PFMVE4 (Figure 3A), a three-peak pattern can be detected which is strongly dependent on the blend composition, i.e., a very small peak (at $w_{FEP} = 0.75$, it is just a poorly detectable shoulder), increasing in extent on increasing the PFMVE4 content, and decreasing in temperature from about −9 to −12 °C, a main peak from about 5 to 3 °C, and a very small shoulder from about 16 to 11 °C, decreasing on increasing PFMVE4 content.

For the blend FEP/PFMVE6 (Figure 3B), a peak with a small shoulder at higher temperature, both decreasing in extent and values on increasing PFMVE6 content, are present.

Last, for the blend FEP/PFMVE10 (Figure 3C), independently upon composition, the typical two-peak pattern of FEP is apparent. However, the peaks appear broader and less resolved on increasing PFMVE10 content. The peak temperatures are nearly the same as those in unblended FEP.

Returning to Tables 2−4, we wish to consider the values of the heats of transition. They are generally located between those of the unblended components and are strongly affected by the blend composition, decreasing on increasing PFMVE content.

In a previous paper,[21] for the blend FEP/PFMVE2, we have shown that melting and crystallization curves present for each composition a single peak, located at an intermediate temperature between those of the neat components. Also, the crystal−crystal transitions are characterized by a main peak at temperatures between those corresponding to the crystalline transitions of the neat components. For the blends with higher contents of FEP, the peak corresponding to the hexagonal−pseudohexagonal transition of FEP can be detected; however, it is very small and shifted to lower temperatures than that in pure FEP.

In Table 5,the calorimetric indexes of crystallinity, $I_{c(DSC)}$, evaluated as $\Delta H_m/\Delta H^o_m$, where ΔH_m is the heat

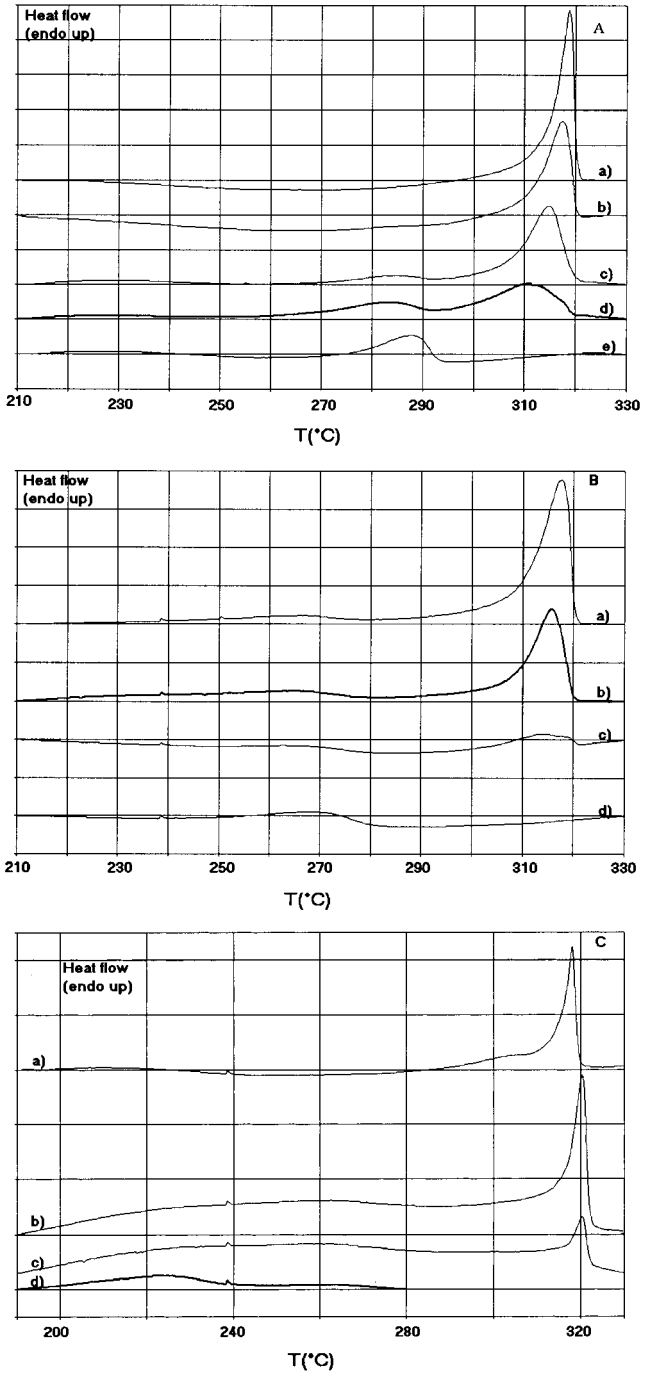

Figure 1. DSC melting traces recorded at 10 °C/min for melt-crystallized (at 10 °C/min) blends at the following compositions: (A) FEP/PFMVE4 at $w_{FEP} = 1.0$ (a), 0.75 (b), 0.50 (c), 0.25 (d), and 0.0 (e); (B) FEP/PFMVE6 at $w_{FEP} = 0.75$ (a), 0.50 (b), 0.25 (c), and 0.0 (d); and (C) FEP/PFMVE10 at $w_{FEP} = 0.75$ (a), 0.50 (b), 0.25 (c), and 0.0 (d).

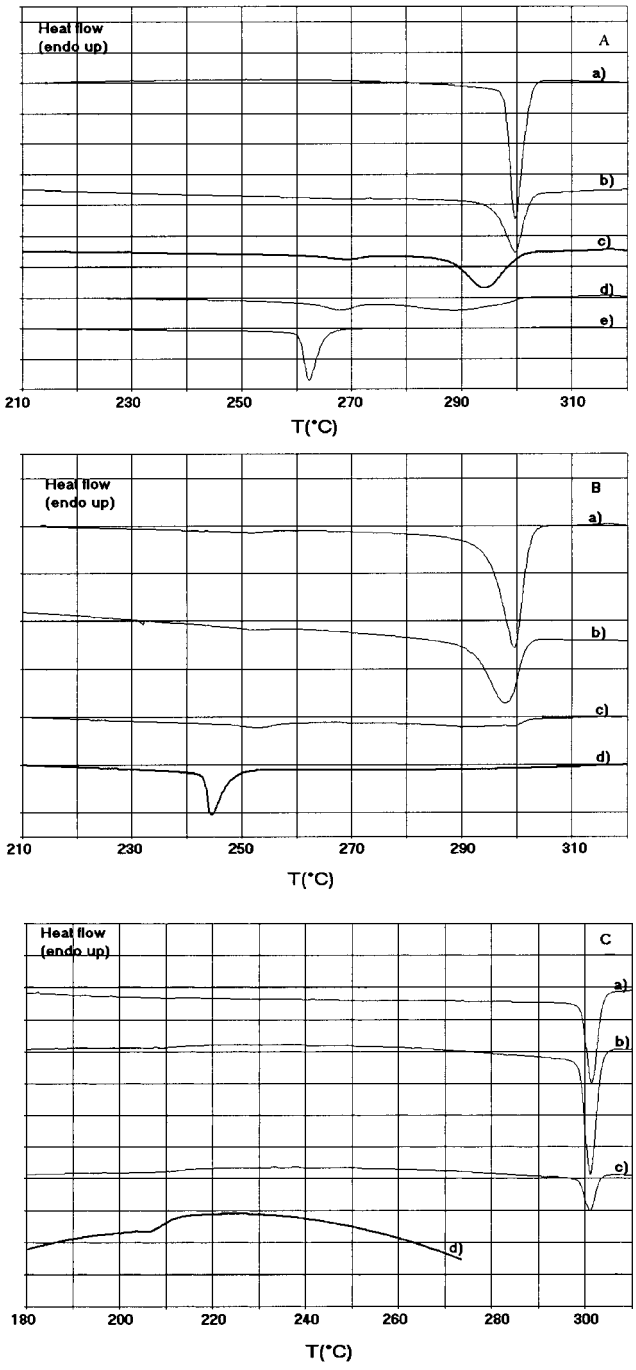

Figure 2. DSC crystallization traces recorded at 10 °C/min for melt-crystallized (at 10 °C/min) blends at the following compositions: (A) FEP/PFMVE4 at $w_{FEP} = 1.0$ (a), 0.75 (b), 0.50 (c), 0.25 (d), and 0.0 (e); (B) FEP/PFMVE6 at $w_{FEP} = 0.75$ (a), 0.50 (b), 0.25 (c), and 0.0 (d); and (C) FEP/PFMVE10 at $w_{FEP} = 0.75$ (a), 0.50 (b), 0.25 (c), and 0.0 (d).

of fusion of the neat components and of the blends and ΔH^{o}_{m} is the heat of fusion of a perfect crystal of PTFE[31] corrected at the equilibrium melting temperatures of copolymers,[26,32] are reported for the unblended copolymers and for the blends with $w_{FEP} = 0.50$.

Another important condition to be fulfilled in order to have chance of cocrystallization is the closeness in the crystallization rate between the components in the mixture.

As proposed by Galante et al.[18] the onset of the first exothermic peak in the DSC curves of crystallization, obtained by cooling at 10 °C/min, taken as the temperature T_o at which the peak starts to deviate from the baseline, may be identified with the crystallization rate of the sample, since it reflects the behavior of the most rapidly crystallizing entity.[33] In Figure 4, we report T_o as a function of PFMVE composition in the blend. For the blend FEP/PFMVE2, the difference in the crystallization rates of the pure components is smaller than in the other cases, and at the same time, the decrease in T_o of the blends, upon increasing the concentration of PFMVE, is larger than those in the other cases.

X-ray Diffraction. In Figure 5, the X-ray diffraction photograph taken with a plate camera at a distance

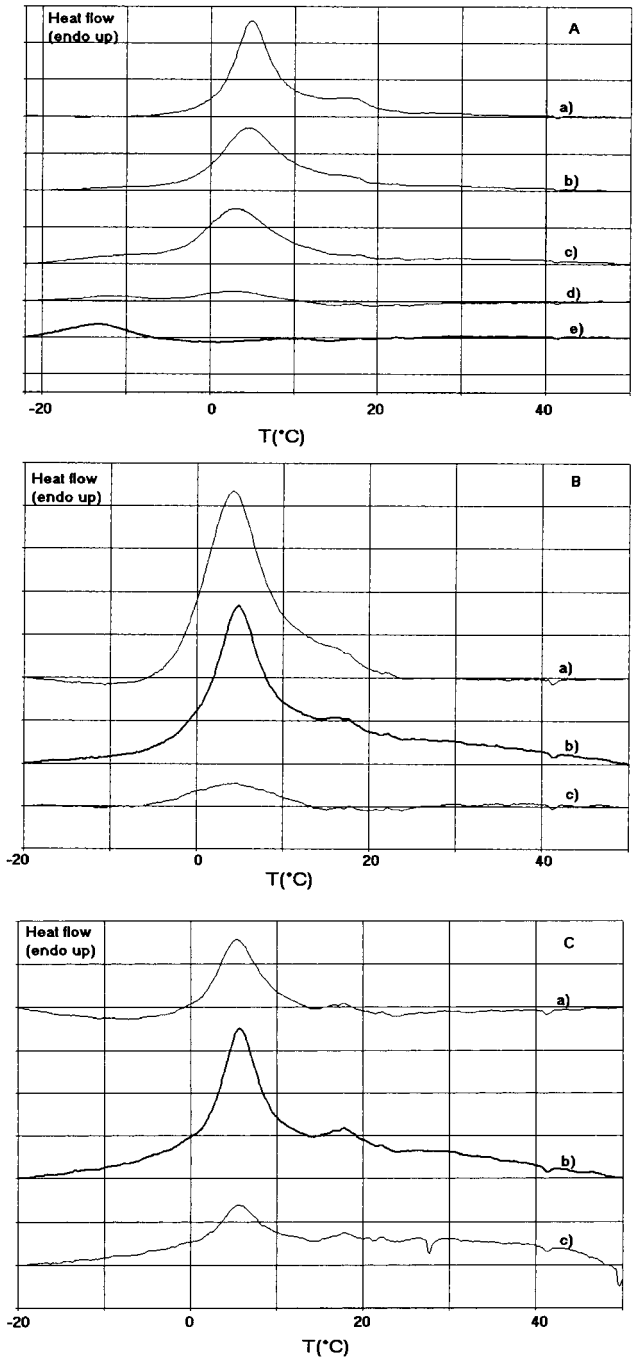

Figure 3. DSC scans recorded at 10 °C/min for melt-crystallized (at 10 °C/min) in the region of crystal−crystal transitions for blends at the following compositions: (A) FEP/PFMVE4 at $w_{FEP} = 1.0$ (a), 0.75 (b), 0.50 (c), 0.25 (d), and 0.0 (e); (B) FEP/PFMVE6 at $w_{FEP} = 0.75$ (a), 0.50 (b), and 0.25 (c); (C) FEP/PFMVE10 at $w_{FEP} = 0.75$ (a), 0.50 (b), and 0.25 (c).

film-sample of 10 mm is reported for FEP. According to the literature,[34,35] an intense reflection (100) located at about $2\theta = 18°$ is observed. The X-ray diffraction photographs of PFMVE copolymers, according to the literature,[36] are very similar and are not reported.

In Figure 6, we report the X-ray diffraction profiles of intensity as a function of 2θ in the range from 10° to 22° for the unblended copolymers and for the melt-crystallized blends with $w_{FEP} = 0.50$, read through a digital imaging reader from photographs such as that of Figure 5. From the Gaussian fitting of these curves (after the subtraction of the amorphous halo), the half-height widths β have been calculated and are reported

Table 5. Angular (2θ) Half-Height Width (β) of the 100 Diffraction Peak, Apparent Crystallite Length (D) in the Direction Perpendicular to the Chain Axis, and Crystallinity Indexes Evaluated from the Experimental X-ray Diffraction Profiles ($I_{C(RX)}$) and from the DSC Curves ($I_{C(DSC)}$) for the Examined Samples[a]

sample	β (deg)		D (Å)		$I_{c(RX)}$ (%)		$I_{c(DSC)}$ (%)
FEP	0.46[a]	0.48[b]	175[a]	168[b]	68[a]	82[b]	76
PFMVE2	0.53	0.55	146	152	44	53	38
Blend $W_{FEP} = 0.50$ FEP/PFMVE2	0.44	0.48	168	190	53	71	53
FEP+PFMVE2	0.48	0.52					
PFMVE4	0.53	0.54	157	149	34	50	18
Blend $W_{FEP} = 0.50$ FEP/PFMVE4	0.49	0.50	164	161	52	60	43
FEP+PFMVE4	0.47	0.51					
PFMVE6	0.56	0.61	144	132	33	34	15
Blend $W_{FEP} = 0.50$ FEP/PFMVE6	0.49	0.53	144	152	43	59	42
FEP+PFMVE6	0.47	0.54					
PFMVE10	0.79	0.97	102	83	17	26	3
Blend $W_{FEP} = 0.50$ FEP/PFMVE10	0.50	0.56	144	143	42	56	35
FEP+PFMVE10	0.47	0.54					

[a] The β values of the peak of the X-ray diffraction profiles obtained by summing the experimental profiles of the neat copolymer samples are also reported. [a] The data in these columns are Lorentz fitted. [b] The data in these columns are Gaussian fitted.

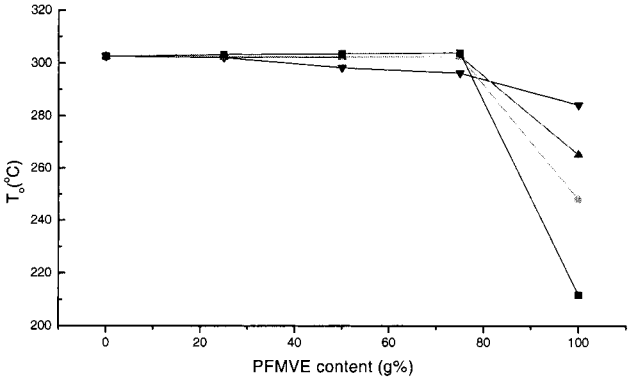

Figure 4. Dependence of the crystallization temperature, T_o, as defined in the text, on composition for blends of FEP with PFMVE containing different comonomer contents: (▼) FEP/PFMVE2, (▲) FEP/PFMVE4, (●) FEP/PFMVE6, and (■) FEP/PFMVE10 blends. Crystallization was carried out by cooling at 10 °C/min from the melt.

in Table 5 (similar results are obtained through the Lorentz fitting and are also reported in Table 5). The value of β increases for the neat copolymers, on increasing the comonomer content. For the blends, the values of β increase on passing from that with PFMVE2 to that with PFMVE10. The correlation lengths D of the crystalline domains, in the direction perpendicular to the chain axes, follow, as expected, the same trend.

In the same table, we also show the diffractometric crystallinity indexes, $I_{c(RX)}$, calculated as the ratio between the area below the crystalline peak and the total area.

They are in a sufficient agreement with the calorimetric crystallinity indexes, $I_{c(DSC)}$, for FEP, PFMVE2, and for the blends, whereas for PFMVE4, PFMVE6, and PFMVE10, the first ones are higher. This discrepancy may be justified by the uncertainty on the value of ΔH^o_m and, more importantly, by the fact that in the evaluation of the calorimetric index the correction due to finite lamellar thickness is not taken into account. It is negligible for FEP and PFMVE2 (and, as a consequence,

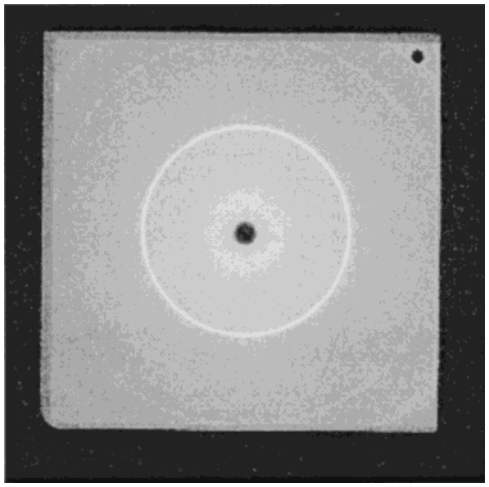

Figure 5. X-ray diffraction photograph taken with a flat-plate camera (distance film-sample 10 mm) for FEP.

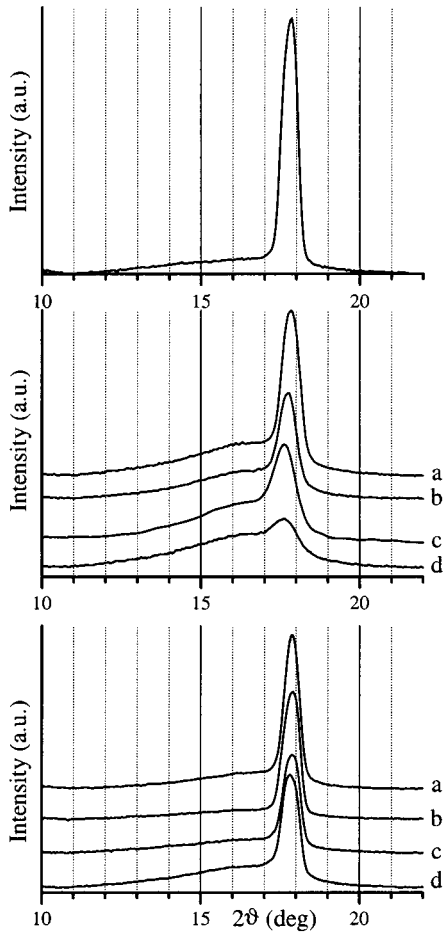

Figure 6. X-ray diffraction profiles of intensity as a function of 2θ read from photographs such as that of Figure 5. (Top) FEP. (Middle) (a) PFMVE2, (b) PFMVE4, (c) PFMVE6, and (d) PFMVE10. (Bottom) Blends with $w_{FEP} = 0.50$ (a) FEP/PFMVE2, (b) FEP/PFMVE4, (c) FEP/PFMVE6, and (d) FEP/PFMVE10.

for the blends, since they all contain FEP) due to their very high lamellar thicknesses, but not for the other samples.

Discussion

Before beginning the discussion about the blends examined in this work, we wish to briefly remind the reader of the conclusions drawn from the calorimetric investigations on the blend between FEP and PFMVE2.[21] The presence of only one calorimetric peak (melting, crystallization, and crystal−crystal transitions), intermediate between those of the unblended components, strongly supports the occurrence of miscibility in the crystal state (cocrystallization).

For the blend FEP/PFMVE4, the dominant peak (melting, crystallization, and crystal−crystal transitions) is strongly dependent on the blend composition, decreasing in value on increasing the lower melting component. In contrast, the lower temperature peak detected in the same curves, which cannot be due solely to the PFMVE4 in the blend, is located at lower temperatures than that in neat PFMVE4. The lowering of the main melting peak may be interpreted by assuming that the more disordered chains of PFMVE4 inhibit the crystallization of FEP. This would be confirmed by the lowering of the temperature of the dominant crystallization peak observed on increasing PFMVE4 content in the blend. The decrease in melting point is due to miscibility in the melt state. Nevertheless, in order for partial cocrystallization to take place, not only the higher melting peak should be shifted to lower temperature but also the lower one should be shifted to higher temperatures. This behavior would be conducive to the production of a unique intermediate peak. In contrast, in our case, the lower melting peak is shifted at even lower temperatures than those in neat PFMVE4. On the other hand, the lower crystallization peak, when present, is much higher than that in neat PFMVE4. Such an increase may be due to chain extension caused by blending, which facilitates easier nucleation.[37] But why in the calorimetric curves is the melting peak of PFMVE4 at lower temperature than that in the neat polymer, whereas the crystallization one is higher? This behavior may be explained by assuming that the low-melting peak could correspond to poor crystals of PFMVE4 (those crystallizing in the tail of the exothermic peak), whereas the best one melts at higher temperature, i.e., in the same region of FEP. Their fusion would occur in lower temperature tail of the dominant peak.

The results concerning the blend FEP/PFMVE6 show a similar, but less pronounced trend, in that the mutual influence of two components is weaker. The lowering of the main melting peak can be explained by taking into account the disturbance induced by PFMVE6 on the crystallization of FEP. On the other hand, the slight increase of the exothermic peak (crystallization of PFMVE6) may be attributed to the chain extension caused by blending, as for the blend with PFMVE4.

For the blend FEP/PFMVE10, the high melting temperature peak is scarcely or not affected by the blend composition. This shows that the poorly crystalline PFMVE10 has no influence on the crystallization of FEP. Moreover, the peaks corresponding to PFMVE10 are hardly detected.

The investigation on the crystallization rate supports the above considerations. In fact, as for polyethylenes,[18] the lowering in the crystallization rate obtained when the difference between the individual T_o's of the components are the lowest could be taken as an indication for cocrystallization, as shown by the other reported results. In the other cases, the difference in T_o values of the blend components is larger, and a negligible influence of PFMVE component on the crystallization

kinetics of FEP is observed. This is in agreement with the smaller and smaller degree of cocrystallization observed on increasing the difference in the defect content of the two components in the mixture.

The calorimetric curves of either melting or crystal−crystal transitions obtained on reheating at 10 °C/min the samples quenched from the melt to −35 °C are very similar to those obtained after crystallization at 10 °C/min; therefore, they are not reported. Nevertheless, in each case, the calorimetric traces are broader and less resolved, in agreement to what was obtained for other blends.[12]

Our results show that FEP and PFMVE copolymers are able to produce cocrystals only when the difference in comonomer content is very low.

The calculation of the solubility parameters of all of the considered polymers, using the group molar attraction constants[38] has been performed in order to have a qualitative indication of the enthalpic contribution to mixing. The commonly used relationship $\delta = \rho(\Sigma F_i/M)$, where ρ is the density of the polymer at the reference temperature, M is the molecular mass of the polymer repeating unit, and F_i is the molar attraction constant in the repeating unit of the polymer, has been modified by us, to be suitable to random copolymers, as $\delta = \rho[(\Sigma F_{iA}/M_A)x_A + (\Sigma F_{iB}/M_B)(1 - x_A)]$, where the subscripts A and B refer to each repeating unit present in the copolymer and x_A is the counit molar fraction. The rough, but close enough, assumption (taking into account the low comonomer content in our copolymers), that the density of the crystalline phase is the same for all copolymers and is equal to that of the homopolymer (2.3 g/cm^3 [29]) is made. The calculation gives

$$\delta_{FEP} = 5.3\ (\text{cal/cm}^3)^{0.5}$$

$$\delta_{PFMVE2} = 5.3\ (\text{cal/cm}^3)^{0.5}$$

$$\delta_{PFMVE4} = 5.4\ (\text{cal/cm}^3)^{0.5}$$

$$\delta_{PFMVE6} = 5.5\ (\text{cal/cm}^3)^{0.5}$$

$$\delta_{PFMVE10} = 5.5\ (\text{cal/cm}^3)^{0.5}$$

For such polymers, where no favorable interactions take place (such as hydrogen bonding), it has been proposed that miscibility would be predictable if the difference in solubility parameters is at most 0.1.[39] Since cocrystallization is an entropy-driven process,[40] similar δ values may suggest possible miscibility in the melt state which is, in this case, indicated only for the blends between FEP and PFMVE2 or PFMVE4. Since the production of cocrystals can take place only from a mixed melt, cocrystallization would be, on this basis, a priori excluded for the other blends. However, to obtain information about the thermodynamics of the liquid state in the melt and to confirm the miscibility in these blends, a work is in progress[41] about the evaluation of the interaction parameter χ, through the determination of the depression of the equilibrium temperatures.[42,43]

The results obtained by X-ray diffraction support the previous considerations. To have a quantitative indication on the possibility of cocrystals formation, in Table 5 the half-height width calculated by the Gaussian (superscripted b column) and Lorentz (superscripted a column) fitting of the sum of the X-ray diffraction profiles of the neat components is reported and compared with that calculated for the corresponding blend. For the blend FEP/PFMVE2, β is lower than the value calculated for the sum FEP+PFMVE2, and it is lower for the other blends. This trend clearly indicates the production of cocrystals only for the blend FEP/PFMVE2 according to the previous calorimetric results.[21]

Conclusions

In this work, we have studied by DSC the phase behavior, in conditions far from equilibrium, of binary blends obtained by melt-mixing of two semicrystalline tetrafluoroethylene random fluorinated copolymers, i.e., FEP and PFMVE. In particular, we have investigated the miscibility of FEP at a single comonomer content and PFMVE at a variable comonomer content. Melting, crystallization, and crystal−crystal transitions show that, on increasing the difference in the defect content of the two copolymers, the miscibility in the crystalline state is hampered and so also in the melt state. However, even when miscibility in the melt is attained, cocrystallization is not a direct consequence, since for cocrystallization the minimum difference of defect concentration is much lower than that of their mixing in the melt state.

The analysis of the crystallization rates gives the same indication: i.e., the closeness of the crystallization rate of each component in the mixture controls the extent of cocrystallization and the data indicate the possibility of cocrystal formation only for FEP and PFMVE2.

A simple calculation of the solubility parameters would indicate possible miscibility in the melt up to a difference in comonomer content of 3 mol %.

The XRD investigation gives further information about the nature of the crystalline phases. Structural modifications, indicative for production of cocrystals, occur for the blend between FEP and PFMVE2.

In conclusion, the ensemble of our results confirm the miscibility in the crystal state only for the blend FEP/PFMVE2, previously suggested through a calorimetric study,[21] whereas in the other, the components give crystal segregation.

Therefore, the miscibility in such blends is essentially governed by the difference in comonomer content between the two components.

Acknowledgment. Professors Gaetano Guerra and Pio Iannelli are gratefully acknowledged for useful advice and stimulating discussions. A MURST grant (Cofin 99 “Interfasi polimeriche e cristallizzazione”) is gratefully acknowledged.

References and Notes

(1) Olabisi, O.; Robeson, L. M.; Shaw, M. T. In *Polymer−Polymer Miscibility*; Academic Press: New York, 1979.
(2) Paul, D. R.; Barlow, J. W. J. *Macromol. Sci. Rev. Macromol. Chem.* **1980**, *18*, 109.
(3) Paul, D. R.; Barlow, J. W. In *Polymer Science and Technology*; Lempner, D., Grisch, K. G., Eds.; Plenum Press: New York, 1980; Vol. 11, p 239.
(4) Runt, J. P.; Martynowicz, L. M. In *Multicomponent Polymer Materials*; Paul, D. R., Sperling, L. H., Eds.; American Chemical Society: Washington, D. C., 1986; Chapter 7, p 111.
(5) Starkweather, H. W. In *Polymer Compatibility and Incompatibility*; Solc, K., Ed.; Harwood: New York, 1982; pp 383−395.
(6) Hu, S. R.; Kyu, T.; Stein R. S. J. *J. Polym. Sci., Part B: Polym. Phys.* **1987**, *25*, 71.

(7) Alamo, R. G.; Flaser, R. H.; Mandelkern, L. *J. Polym. Sci., Part B: Polym. Phys.* **1988**, *26*, 2169.
(8) Martinez Salazar, J.; Sanchez Cuesta, M.; Plans, J. *Polymer* **1991**, *32*, 2984.
(9) Hill, M. J.; Barham, P. J.; Keller, A. *Polymer* **1992**, *33*, 2530.
(10) Tashiro, K.; Izuchi, M.; Kobayashi, M.; Stein, R. S. *Macromolecules* **1994**, *27*, 1221.
(11) Natta, G.; Allegra, G.; Bassi, I. W.; Sianesi, D.; Caporiccio, G.; Torti, E. *J. Polym. Sci., Part A: Polym. Chem.* **1965**, *3*, 4263.
(12) Guerra, G.; Karasz, F. E.; MacKnight, W. J. *Macromolecules* **1986**, *19*, 1935.
(13) Tanaka, H.; Lovinger, A. J.; Davis, D. D. *J. Polym. Sci., Part B: Polym. Phys.* **1990**, *28*, 2183.
(14) Runt, J.; Jin, L.; Talibuddin, S.; Davis, C. R. *Macromolecules* **1995**, *28*, 2781.
(15) Hill, M. J.; Barham, P. J.; Keller, A.; Rosney, C. C. A. *Polymer* **1991**, *32*, 1384.
(16) Hill, M. J.; Barham, P. J.; Keller, A.; Rosney, C. C. A. *J. Mater. Sci. Lett.* **1988**, *7*, 1271.
(17) Alamo, R. G.; Londono, J. D.; Mandelkern, L.; Stehling, F. C.; Wignall, G. D. *Macromolecules* **1994**, *27*, 411.
(18) Galante, M. J.; Mandelkern, L.; Alamo, R. G. *Polymer* **1998**, *21*, 5105.
(19) Datta, J.; Nandi, A. K. *Polymer* **1994**, *35*, 4804.
(20) Datta, J.; Nandi, A. K. *Polymer* **1996**, *37*, 5179.
(21) Pucciariello, R.; Angioletti, C. *J. Polym. Sci., Part B: Polym. Phys.* **1999**, *37*, 679.
(22) Pucciariello, R. *J. Polym. Sci., Part B: Polym. Phys.* **1994**, *32*, 1771.
(23) Pucciariello, R. *J. Polym. Sci., Part B: Polym. Phys.* **1996**, *34*, 1751.
(24) Pucciariello, R.; Villani, V. *Thermochim. Acta* **1993**, *227*, 145.
(25) Pucciariello, R.; Mancusi, C. *J. Appl. Polym. Sci.* **1999**, *73*, 919.
(26) Pucciariello, R.; Villani, V.; Mancusi, C. *J. Appl. Polym. Sci.* **1999**, *74*, 1607.
(27) Morgan, R. A. European Patent 191605 1986.
(28) Bunn, C. W.; Howells, E. R. *Nature* **1954**, *174*, 549.
(29) Sperati, C. A.; Starkweather, H. W. *Adv. Polym. Sci.* **1961**, *2*, 465.
(30) Weeks, J. J.; Sanchez, I. C.; Eby, R. K.; Poser, I. C. *Polymer* **1980**, *21*, 325.
(31) Lau, S. F.; Suzuki, H.; Wunderlich, B. J. *Polym. Sci., Part B: Polym. Phys.* **1984**, *22*, 379.
(32) Pucciariello, R. *J. Appl. Polym. Sci.* **1997**, *64*, 409.
(33) Tashiro, K.; Imanishi, K.; Izuchi, Y.; Kobayashi, M.; Kobayashi, K.; Satoh, M.; Stein, R. S. *Macromolecules* **1995**, *28*, 8477.
(34) Bolz, L. G.; Eby, R. K. *Res. Nat. Bur. Stand.* **1965**, *69A*, 481.
(35) Weeks, J. J.; Eby, R. K.; Clark, E. S. *Polymer* **1981**, *22*, 1496.
(36) Guerra, G.; Venditto, V.; Natale, C.; Rizzo, P.; De Rosa, C. *Polymer* **1998**, *39*, 3205.
(37) Huang, J.; Prassad, A.; Marand, H.; Roitman, D. B. *Polymer* **1994**, *35*, 1896.
(38) Hoy, K. J. *Paint Technol.* **1970**, *3*, 71.
(39) Coleman, M. M.; Serman, C. J.; Bhagwagar, D. E.; Painter, P. C. *Polymer* **1990**, *31*, 1187.
(40) Datta, J.; Nandi, A. K. *Macromol. Chem. Phys.* **1998**, *199*, 2583.
(41) Pucciariello, R.; Villani, V., work in progress.
(42) Flory, P. J. *Principles of Polymer Chemistry*; Cornell University Press: Ithaca, NY, 1953.
(43) Nishi, T.; Wang, T. T. *Macromolecules* **1975**, *8*, 909.

MA001172J